

Vertical transport and electroluminescence in InAs/GaSb/InAs structures: GaSb thickness and hydrostatic pressure studies

M. Roberts, Y. C. Chung, S. Lyapin, N. J. Mason, R. J. Nicholas, and P. C. Klipstein

Department of Physics, Oxford University, Clarendon Laboratory, Parks Road, Oxford OX1 3PU, United Kingdom

(Received 27 September 2001; revised manuscript received 11 March 2002; published 19 June 2002)

We have measured the current-voltage (I - V) of type-II InAs/GaSb/InAs double heterojunctions (DHET's) with "GaAs like" interface bonding and GaSb thickness between 0 and 1200 Å. A negative differential resistance (NDR) is observed for all DHET's with GaSb thickness >60 Å below which a dramatic change in the shape of the I - V and a marked hysteresis is observed in some samples. The temperature dependence of the I - V is found to be very strong below this critical GaSb thickness. The I - V characteristics of selected DHET's are also presented under hydrostatic pressures up to 11 kbar. Finally, a midinfrared electroluminescence is observed at 1 bar with a threshold at the NDR valley bias. The band profile calculations presented in the analysis are markedly different to those given in the literature and arise due to the positive charge that it is argued will build up in the GaSb layer under bias. We conclude that the dominant conduction mechanism in DHET's is most likely to arise out of an inelastic electron-heavy-hole interaction similar to that observed in single heterojunctions with "GaAs like" interface bonding, and not out of resonant electron-light-hole tunneling as proposed by Yu *et al.* A Zener tunneling mechanism is shown to contribute to the background current beyond NDR.

DOI: 10.1103/PhysRevB.65.235326

PACS number(s): 73.40.Gk, 73.50.-h

I. INTRODUCTION

There has been considerable interest recently in resonant tunneling devices involving coupling between the conduction and valence bands of different materials across heterointerfaces. Much of this study has focused on InAs/GaSb/AlSb structures owing to the "broken-gap" band alignment at the InAs/GaSb interface. Devices exploiting the strong interband coupling shown in these structures include resonant tunneling diodes¹ and interband cascade lasers.² Despite rapid progress and extensive modeling, the details of the conduction mechanisms in even the simplest structures still remain poorly understood. Following a detailed study of the conduction in InAs/GaSb single heterojunctions³ (SHET's), where hydrostatic pressure was used to vary the band overlap and hence the interband coupling, this work investigates the case of the InAs/GaSb/InAs double heterojunction (DHET), shown by the band profile in Fig. 1. Both SHET's and DHET's show a region of negative differential resistance in their I - V characteristics and abnormally high background currents of unconfirmed origin beyond the negative differential resistance (NDR).

The NDR arising out of interband coupling in single-barrier structures was proposed⁴ and demonstrated⁵ by Chow *et al.* for the staggered lineup HgCdTe/CdTe/HgCdTe DHET, and subsequently by Beresford *et al.*,⁶ Munekata *et al.*,⁷ and Söderström *et al.*⁸ from InAs/AlGaSb/InAs DHET's. The NDR in this case can be explained by consideration of the imaginary wave vector of the tunneling electrons in the barrier region using a two-band electron-light-hole $\mathbf{k}\cdot\mathbf{p}$ model.⁹ This shows that the tunneling initially becomes more difficult with increasing bias as electrons strike the barrier with energies further from the barrier valence-band edge. NDR was subsequently observed in a broken-gap InAs/GaSb/InAs DHET by Taira *et al.*,¹⁰ who suggested that the current trans-

port mechanism was Ohmic conduction from one InAs electrode to the other through the GaSb valence band, which is cut off at higher bias by GaSb band-gap blocking. A similar characteristic was observed by Luo *et al.*¹¹ a year later and interpreted in terms of conduction through transmission resonances arising out of the mixing between InAs conduction-band and GaSb valence-band states. Further investigation into the GaSb thickness dependence of the I - V by Yu *et al.*¹² showed that the NDR is lost as the GaSb thickness is reduced below 60 Å. According to their calculations this loss in NDR coincides with the loss in the electron-light-hole overlap at the flat band. This led the authors to conclude that the NDR arises out of a resonant electron-light-hole tunnel current and that the heavy holes contribute only weakly to the conduction. More detailed theoretical models have since been presented in support of this conclusion, where electron-heavy-hole coupling considerations are shown to only give

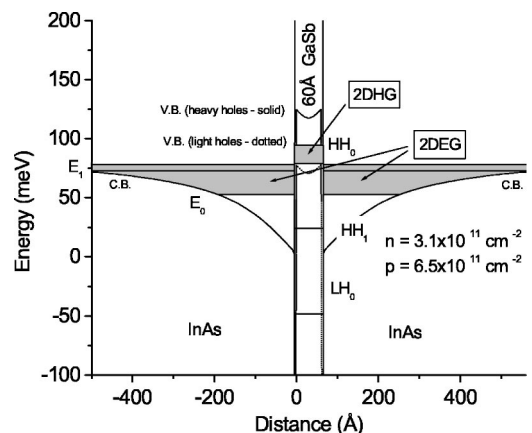


FIG. 1. Equilibrium band profile of a 60 Å GaSb DHET with undoped layers at 0 K, showing the two-dimensional 2D carrier density in the two-electron and one-hole layers.

rise to secondary features in the theoretical I - V characteristic.¹³

However, there are reports in the literature where the results are difficult to interpret using the resonant electron–light-hole tunneling model. Takamasu *et al.*¹⁴ have applied magnetic fields parallel to the interfaces of InAs/GaSb/InAs DHET’s showing NDR, where the peak NDR bias gives the opposite behavior to that predicted. A detailed study of the conduction mechanisms in the related InAs/GaSb SHET structures by Khan-Cheema *et al.*³ has shown that the interface bonding (“InSb like” or “GaAs like”) plays a very important role in the conduction and that the NDR in the “GaAs” case is more likely to arise out of an inelastic electron–heavy-hole interaction. The temperature^{15,16} and barrier composition dependence¹⁷ of the valley current suggest the possibility of light-hole (LH) tunneling into the emitter valence band at biases above 400 mV, although this has not yet been observed directly.

In all cases, the modeling is strongly dependent on the value taken for the band overlap, which is believed to lie in the range 125–155 meV and is dependent on the interface bonding.¹⁸ None of the reports in the literature include the effects of strain on the heavy- and light-hole valence-band edges, which we believe to be significant as it decreases the energy of the LH levels an additional 47 meV below those of the HH. The band profile models are also very sensitive to the treatment of charge buildup in the self-consistent potentials on either side of the type-II interface. Simple models assume a 3D emitter distribution, despite reports of the 2D nature of the confinement.^{7,19} Positive-charge buildup in the GaSb is also ignored in the analysis of Yu *et al.*¹² However, the observation of intrinsic bistability in an InAs/AlGaSb/InAs/AlGaSb/InAs double-barrier structure²⁰ strongly suggests that both positive- and negative-charge buildup must be included in any realistic analysis of conduction in this family of devices.

In this work, we present vertical transport results on metal-organic vapor phase epitaxy (MOVPE) grown DHET’s with “GaAs-like” interfaces over a wider range of GaSb layer thickness (0–1200 Å) than reported by Yu *et al.*¹² The results from thicker GaSb layers are qualitatively similar to those given in the literature, but here we report the first observation of a dramatic drop in the conductance for DHET’s with GaSb thickness <60 Å. DHET’s in this regime are shown to behave dramatically differently to those with GaSb thickness >60 Å. Hydrostatic pressures of up to 11 kbar allow the continuous tuning of the band overlap and thus the relative electron and hole subband alignments. This allows the electron-light-hole resonance to be pushed below the region of band overlap and its role in the conduction to be more carefully assessed than can be done by GaSb thickness dependence studies alone. An interband electroluminescence is also observed with a threshold at the NDR valley bias. This provides the first direct evidence of the nature of the background conduction mechanism in these structures, previously of unconfirmed origin.

We also present self-consistent calculations of the band profiles to compare with our results. Our profiles appear to be dramatically different to those found in the literature.¹³

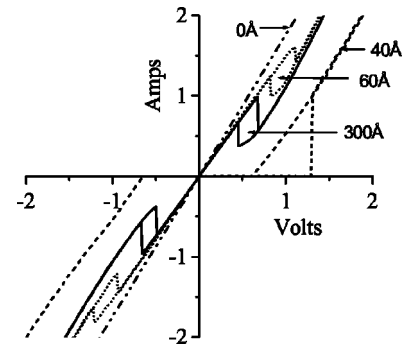


FIG. 2. I - V characteristics of InAs/GaSb/InAs DHET’s with different GaSb widths at 77 K.

We argue that this discrepancy has its origins in the significant 2D hole concentration that accumulates in the central GaSb layer. Analysis of the thickness and hydrostatic pressure dependence of the conduction using this model provides an adequate explanation for the midinfrared emission beyond NDR and also gives strong evidence against the resonant electron–light-hole tunneling theory of Yu *et al.*¹² Although the alignment of the light-hole subband is shown to be important, it appears more likely that the conduction arises out of an inelastic interaction between the electrons and heavy holes, more similar to that reported for SHET’s with “GaAs-like” interfaces.³

II. EXPERIMENTAL DETAILS

n -InAs/ p -GaSb/ n -InAs nominally undoped DHET’s were grown on nominally undoped n -InAs substrates with GaSb layer thicknesses of 0–1200 Å, followed by a 3000-Å InAs cap. The interface bonding was biased to be “GaAs-like” using a shutter sequence similar to that described elsewhere.²¹ The layer thicknesses were calibrated by monitoring the Fabry-Perot oscillations in the surface photoabsorption (SPA) signal during deposition.²¹

The wafers were processed into 150 μm mesa structures and metalized with thermally evaporated, nonannealed Cr/Au pads. Here 3–20 μsec pulsed I - V and electroluminescence were measured at temperatures of 25–300 K. Pulsed I - V measurements were also carried out under hydrostatic pressures up to 11 kbar using a pressure cell as described elsewhere.²² All DHET’s showing NDR were highly sensitive to a small series parasitic resistance which was always present due to contact resistances of $\leq 1 \Omega$. This parasitic resistance could be estimated fairly accurately and its effects removed by calculating its two limiting values. Too high a value gives rise to a negative slope in the high-current post-NDR region while too low a value leads to a peak bias lying above the valley. Thus, for example, the parasitic resistance for the 300 Å DHET in Fig. 2 was found to be in the range $0.30 \pm 0.05 \Omega$.

III. EXPERIMENTAL RESULTS

A. GaSb width dependence of I - V

The I - V results at 77 K as a function of GaSb thickness are presented in Fig. 2. The hysteresis in the NDR is a result

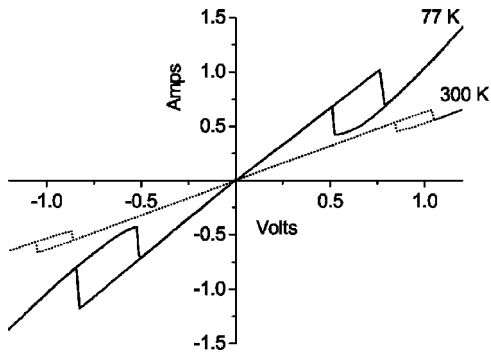


FIG. 3. *I-V* characteristics of a 150 Å GaSb DHET at 77 K and 300 K.

of the large current densities characteristic of these structures making the effects of parasitic resistance significant as already mentioned in Sec. II. As a result, the voltage shown does not represent the voltage across the DHET alone but includes that across the parasitic resistance. However, the peak and valley current densities are unaffected by the parasitic resistance. These are found to scale with the cross-sectional mesa area as would be expected for negligible surface leakage currents. The *I-V* traces are only weakly dependent on the GaSb thickness for GaSb thicknesses above 60 Å, showing a slight decrease in peak and valley currents for wider structures, similar to the results reported by Yu *et al.*¹² For GaSb thickness below 60 Å, the *I-V* trace changes dramatically. This is most remarkable for the 40 Å GaSb DHET example shown, where the NDR is lost entirely at 77 K and the current densities at low bias are reduced by three orders of magnitude. Similar characteristics were also observed for structures with GaSb thicknesses of 20, 30, and 50 Å, some showing a marked hysteresis, and others none. The hysteresis shown in Fig. 2, which is also observable under dc biasing, is not thought to be an effect of the parasitic resistance as the device resistance is now much higher. At the switching point the current density increases abruptly by three orders of magnitude. The 0 Å control sample and the 10 Å GaSb DHET give an Ohmic characteristic.

B. Temperature dependence of *I-V*

The temperature dependence for two DHET's with 150 Å and 40 Å of GaSb are shown in Figs. 3 and 4, respectively.

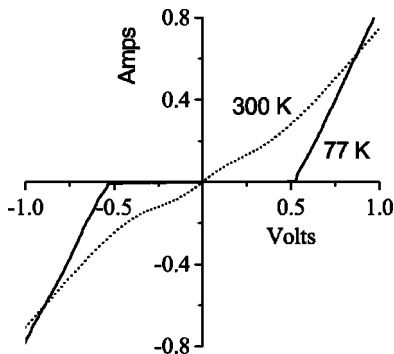


FIG. 4. *I-V* characteristics of a 40 Å GaSb DHET at 77 K and 300 K.

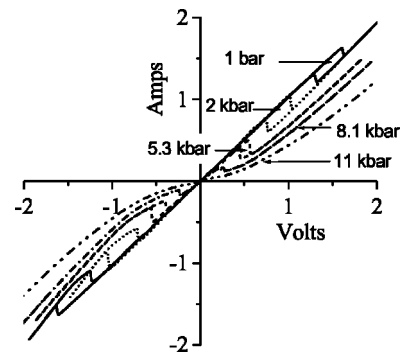


FIG. 5. *I-V* characteristics of a 60 Å GaSb DHET at 77 K as a function of hydrostatic pressure.

The temperature dependence for DHET's with GaSb thickness >60 Å is weak, where the NDR is found to persist, as was the case for SHET's with "GaAs-like" interfaces.³ The shift along the voltage axis is a result of changes in the parasitic resistance with temperature, confirmed by the 0 Å GaSb control sample and consistent with reports in the literature. In contrast, the temperature dependence for DHET's with GaSb thickness <60 Å is much stronger. The dramatic suppression of the low bias conductance in this regime is lifted at higher temperatures, with a weak NDR feature returning around 200 mV at 300 K.

C. Hydrostatic pressure dependence of *I-V*

The evolution of the *I-V* traces under hydrostatic pressure is shown in both types of structure in Fig. 5 for the 60 Å GaSb DHET and in Fig. 6 for the 50 Å GaSb DHET. The NDR feature for the 60 Å GaSb DHET moves continuously towards zero and is still discernible at 11 kbar. For the thinner structures, the onset of conduction increases from ~500 mV to ~750 mV between 1 bar and 11 kbar, after which the slope conductances are very similar. The current axis is expanded in Fig. 7 to reveal the strong suppression of the low bias conductance with pressure for this structure.

D. Electroluminescence results

Mid-IR electroluminescence is also detected with a threshold at the NDR valley bias for all the structures show-

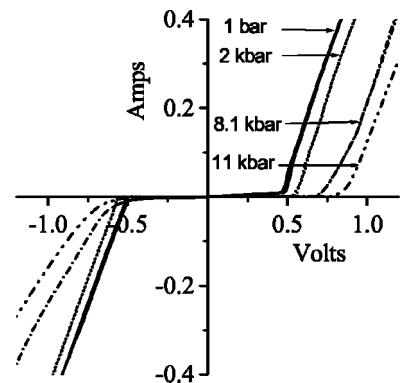


FIG. 6. *I-V* characteristics of a 50 Å GaSb DHET at 77 K as a function of hydrostatic pressure.

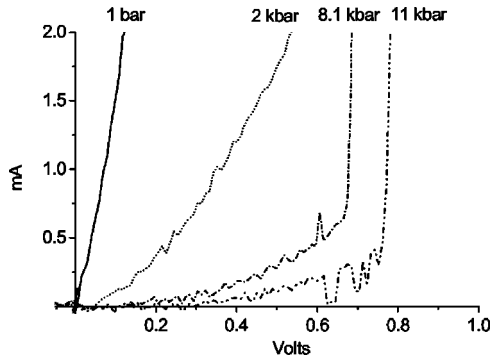


FIG. 7. I - V characteristics of a 50 Å GaSb DHET at 77 K as a function of hydrostatic pressure expanded at low currents.

ing NDR, as shown for example by the 150 Å DHET in Fig. 8. The 30 K electroluminescence spectrum corresponds to that of bulk InAs photoluminescence (peak at 410 meV or $3.02 \mu\text{m}$), as shown in Fig. 9. The slight redshift in the electroluminescence spectrum is attributed to Joule heating effects. A similar emission is observed beyond 500 mV for the 40 Å DHET.

IV. BAND PROFILE CALCULATIONS

Analysis of these results requires careful modeling of the band profiles and subband energy levels both under equilibrium and nonequilibrium conditions. Self-consistent calculations on DHET structures in the literature,^{13,23} ignore any confinement effects in the emitter and use the 3D Thomas-Fermi approximation to relate the Fermi level to the band edges. Also, the band overlap appears to be independent of strain and interface bonding, which we believe will have a dramatic effect on the band profile calculations.

In our work, the emitter and collector are treated as 2D wells for electrons, and the GaSb layer is treated as a 2D well for light and heavy holes, consistent with the true band bending expected for a type-II interface. As a first approximation, each layer in this three-layer system is assumed to be in local thermal equilibrium, allowing a quasi-Fermi level to be defined in each. Each layer is solved self-consistently using a transfer matrix technique, under the assumption of total charge neutrality across the whole structure. The band profile

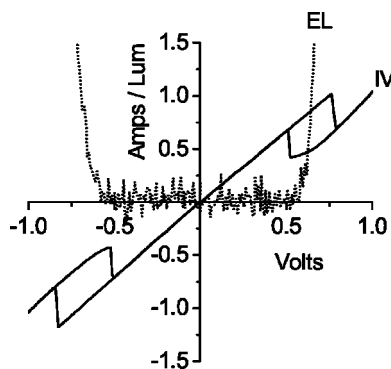


FIG. 8. I - V and electroluminescence characteristics of a 150 Å GaSb DHET at 30 K.

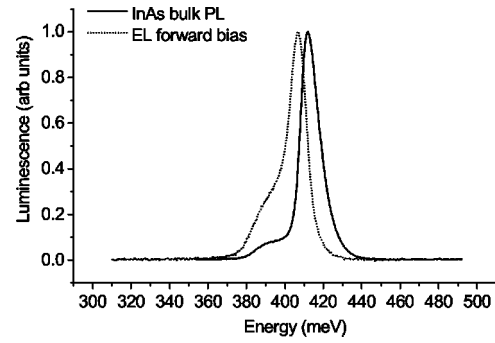


FIG. 9. Photoluminescence and electroluminescence spectrum of a 150 Å GaSb DHET at 30 K.

solved in this way for a 60 Å GaSb DHET at equilibrium is shown in Fig. 1. The band offset is taken as 125 meV for the heavy holes,^{3,18} and the light-hole offset is lowered by ~ 47 meV as the GaSb is under biaxial compression. Similar band profiles and experimental evidence for the 2D nature of the electrons in the contact regions has been provided in an analogous structure by Gonzalez *et al.*¹⁹

Solving the band profile under nonequilibrium conditions requires a much more complex analysis, as inelastic processes and nonequilibrium Fermi distributions must be included in a realistic model. In the analysis by Yu *et al.*,¹² all inelastic processes are ignored and charge buildup in the GaSb under biased conditions appears to be negligible, resulting in potential profiles with a uniform electric field in the GaSb region. In this work, the model used for the equilibrium band profiles is adapted to give trial solutions under bias, which can include both the confinement effects in the contact regions as well as the effects of positive charge buildup in the central layer. Self-consistent solutions correspond to cases where the quasi-Fermi level of the holes in the GaSb lies in between those of the contacts. The nonequilibrium band profile is found to be very sensitive to the corresponding charge distributions. One limiting solution gives band profiles very similar to those found in the analysis of Yu *et al.*,¹² where the Fermi level is broken at the collector interface and a depletion region is formed at the collector contact. At the other extreme, the band profile is shown in Fig. 10 and resembles that given by Lapushkin *et al.*²⁴ in the modeling of similar structures with AlSb barriers. In this case the Fermi level is broken at the emitter contact, resulting in a significant buildup of holes in the GaSb and an accumulation region in the collector contact.

We point out that the first solution is highly unstable against the rapid leakage of GaSb valence electrons into the InAs conduction band at the $+ve$ electrode and that the more likely solution will resemble the band profile shown in Fig. 10. This follows from estimates of the light-hole quasi-bound-state lifetime,¹³ which is predicted to be extremely short, of the order of a few tens of femtoseconds for GaSb widths around 60–100 Å. This quasi-bound-state lifetime is related to the width of the electron–light-hole transmission resonance, which is found to be much broader than for typical quasibound states in more conventional double-barrier layers. This short lifetime will promote the buildup of posi-

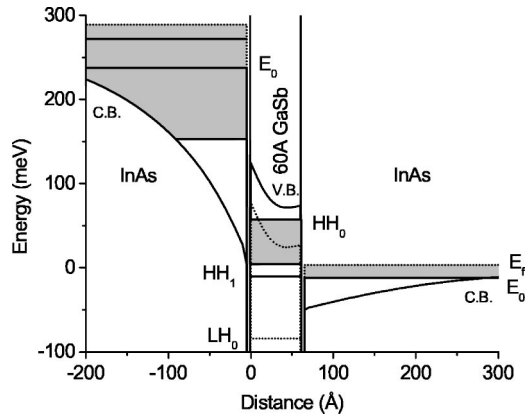


FIG. 10. Band profile of 60 Å GaSb DHET at 285 mV, close to the estimated NDR peak bias across the structure. The shaded regions show the occupied states in each of the layers which are each supposed to be in thermal equilibrium with a quasi-Fermi level.

tive charge in the central layer until the GaSb and collector contact quasi-Fermi levels are close to equilibrium, as is the case for all the band profiles shown in this work.

Hole dispersions were calculated using a four-band $\mathbf{k} \cdot \mathbf{p}$ model to give insight into the effects of valence-band mixing. It turns out that the large density of states offered by the flattening of the HH_0 dispersion results in only the HH_0 subband being occupied. Consequently, the light-hole resonance will not fall between the contact Fermi levels in any of the cases studied. This treatment therefore precludes any coherent tunneling mechanism through the electron–light-hole resonance, in contrast to the theory of Yu *et al.*¹²

V. DISCUSSION

We begin with the 3 μm luminescence observed in all samples at biases >400 mV. This is explained by the onset of Zener tunneling, which coincides with the NDR valley bias at ambient pressure. Once the contact quasi-Fermi levels are separated in energy by more than the InAs band gap, valence electrons in the emitter can tunnel into the conduction band of the $+ve$ contact. This explanation is consistent with the band profiles suggested in this work, corresponding to that shown in Fig. 11. This observation shows clearly that this elastic Zener tunneling mechanism contributes significantly

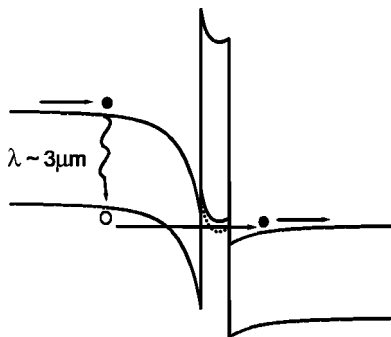


FIG. 11. Band profile of a 150 Å GaSb DHET at 500 mV showing Zener tunneling mechanism and accompanying electroluminescence.

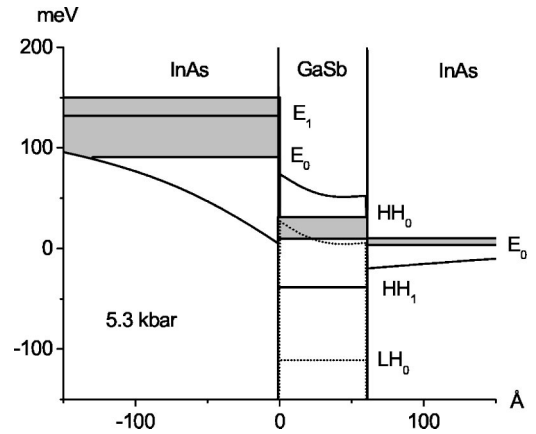


FIG. 12. Band profile of a 60 Å GaSb DHET at 141 mV under 5.3 kbar, close to the estimated NDR peak bias across the structure.

to the background current in these structures, previously of unconfirmed origin.

The peak NDR bias at 1 bar is now estimated and compared to nonequilibrium band profiles to determine the nature of the peak NDR conduction mechanism. The bias across the 60 Å DHET from Fig. 5 is estimated at ~ 285 mV after subtracting an estimated parasitic resistance of 0.8Ω using the method described above. This is consistent with the results from DHET's in the literature where parasitic resistances are less dominant. The band profile given in Fig. 10 shows that under these conditions the lowest electron subband is far from being resonant with any of the hole subbands. The electron and hole ground states are separated by over ~ 100 meV, suggesting that an inelastic process is responsible for the NDR. This is in agreement with the analysis of NDR in “GaAs-like” SHET's reported previously.³ Although the light holes do not appear to be resonant with the emitter electron distribution, their proximity will nevertheless have the effect of increasing the penetration of the electron wave function into the GaSb through electron–light-hole mixing. Similarly, the penetration of the heavy holes at finite k_{\parallel} into the InAs will be enhanced by the proximity of the light-hole subband. The resulting electron–heavy-hole wave function overlap will therefore be significant in this case and allow an appreciable inelastic current to flow. Further increase in the bias will result in a greater energy separation of the electrons and holes and a stronger attenuation of the wave function tails into the GaSb, at which point the region of NDR is observed.

The hydrostatic pressure results for the 60 Å GaSb DHET are consistent with this interpretation and provide conclusive evidence that the NDR does not arise out of resonant conduction through the light-hole subband. Hydrostatic pressure increases the bulk band gaps and decreases the band overlap at ~ 10 meV/kbar,²⁵ resulting in a lowering of the light-hole subband energy. At 5.3 kbar a clear NDR is observed despite the energy of the light-hole subband being unambiguously below the region of band overlap, as shown in Fig. 12.

As the band overlap decreases with pressure, the charge transfer across the interface also decreases, resulting in a change in shape of the self-consistent potential and a lowering of the confined electron subbands. This results in a re-

duced bias to achieve the same electron-hole energy separation, hence the decrease observed in the NDR position with increasing pressure (Fig. 5) and the decrease in peak current. The peak NDR position analysis of the band profiles for all of the pressures studied shows that the electrons and heavy holes are always uncrossed by ~ 50 – 100 meV at the peak bias, again consistent with an inelastic conduction mechanism.

We now turn to the dramatically reduced conduction in structures with GaSb layers of 50 Å and less. The fact that hydrostatic pressure does not induce similar behavior in the 60 Å and wider structures shows that the electron-hole level alignment and overlap is much more strongly affected by confinement than by pressure once the GaSb width is reduced below 60 Å. This is indeed confirmed by the band profile calculations, where the light-hole ground state is lowered by over 120 meV as the GaSb width changes from 80 to 40 Å whereas the electron subband energy is hardly affected. This explains the dramatic change in conduction observed, which we argue is a result of the dramatically reduced electron-hole overlap as the light-hole energy is decreased. Application of hydrostatic pressure further decreases the overlap as expected, and is reflected in the reduction in current density in Fig. 7.

Moreover, the reappearance of a weak resonant feature at 1 bar at 300 K provides additional evidence for the inelastic nature of the conduction in these structures. The increase in temperature gives the opposite effect to pressure, with the band overlap increasing by around 30 meV between 77 and 300 K²⁶ resulting in a raising of the light-hole subband relative to the emitter electron distribution. Furthermore, the higher temperature will allow holes to populate higher subbands with more light-hole character and greater penetration. The resulting enhanced electron-hole overlap then gives rise to an increase in the conductivity and even a weak NDR, as observed.

Finally, we consider the intrinsic bistability shown in many of the samples studied, where the conduction is found in some cases to abruptly switch by over three orders of magnitude. This strongly suggests that there are two different steady-state charge distributions at a given bias, and we propose that these correspond to there being different amounts of positive charge accumulation in the GaSb, in some ways similar to that proposed by Chow *et al.*²⁰ A schematic pair of band profiles to show the two different states of the system is shown in Fig. 13 where the mechanism for the enhanced current is related to a resonant interband tunneling via the light hole. Although a significant positive charge buildup is very likely in the thicker structures, it is feasible that this is not always the case for thinner structures. The efficient leakage of electrons from the GaSb valence band into the positive contact could indeed become more difficult for thinner structures as the light-hole subband is pushed to lower ener-

40 Å GaSb DHET 510mV

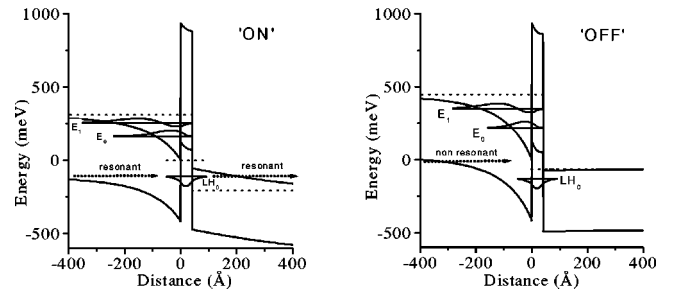


FIG. 13. Band profile of a 40 Å GaSb DHET at 510 mV bias showing two possible band profiles corresponding to the on and off states in the thin layer structures.

gies and conduction is turned off. When the GaSb barrier becomes even thinner, direct electron tunneling may begin to occur.

The conduction mechanisms must be dramatically different in the two bistable configurations to give such radically different current densities, clearly demonstrating the sensitivity of these structures to the band profile models used.

VI. CONCLUSIONS

We have presented a detailed investigation into the nature of the conduction in InAs/GaSb/InAs DHET's. A dramatic drop in the conductance, a loss in the NDR, and a marked intrinsic hysteresis is observed for DHET's with GaSb thickness < 60 Å. The thickness and hydrostatic pressure dependence of the conduction are interpreted with the help of self-consistent band profiles, where the inclusion of a significant positive-charge buildup in the GaSb is found to give solutions quite different to those found in the literature. Resonant electron–light-hole tunneling is shown not to be the dominant transport mechanism, although the position of the light-hole subband is believed to be important in determining the degree of electron-hole overlap necessary for conduction. Inelastic conduction involving electrons and heavy holes is most likely to be the dominant process at the peak NDR bias, similar to the conduction mechanism proposed for the InAs/GaSb SHET's with “GaAs like” interface bonding.³ The hysteresis observed in many of the DHET's with thinner GaSb layers demonstrates that the conduction is very sensitive to the steady-state charge distribution. An interband luminescence observed beyond NDR is explained by Zener tunneling, confirming an important contribution to the background conduction mechanism.

ACKNOWLEDGMENT

We are grateful to the EPSRC (UK) for the support of this work.

¹J.R. Söderström, D.H. Chow, and T.C. McGill, *Appl. Phys. Lett.* **55**, 1094 (1989).

²C.H. Lin, R.Q. Yang, D. Zhang, S.J. Murry, S.S. Pei, A.A. Allerman, and S.R. Kurtz, *Electron. Lett.* **233**, 598 (1997).

³U.M. Khan-Cheema, P.C. Klipstein, and N. Mason, *Proc. ICPS* **23**, 2271 (1996); P.C. Klipstein, *Semicond. Semimetals* **55**, 45 (1998).

⁴D.H. Chow and T.C. McGill, *Appl. Phys. Lett.* **48**, 1485 (1986).

- ⁵D.H. Chow, T.C. McGill, I.K. Sou, J.P. Faurie, and C.W. Nieh, *Appl. Phys. Lett.* **52**, 54 (1987).
- ⁶R. Beresford, L.F. Luo, and W.I. Wang, *Appl. Phys. Lett.* **54**, 1899 (1989).
- ⁷H. Munekata, T.P. Smith, and L.L. Chang, *J. Vac. Sci. Technol. B* **7**, 324 (1989).
- ⁸J.R. Söderström, D.H. Chow, and T.C. McGill, *Appl. Phys. Lett.* **55**, 1348 (1989).
- ⁹J. Heremans, D.L. Partin, and P.D. Dresselhaus, *Appl. Phys. Lett.* **48**, 644 (1986).
- ¹⁰K. Taira, I. Hase, and H. Kawai, *Electron. Lett.* **25**, 1708 (1989).
- ¹¹L.F. Luo, R. Beresford, K.F. Longenbach, and W.I. Wang, *J. Appl. Phys.* **68**, 2854 (1990).
- ¹²E.T. Yu, D.A. Collins, D.Z. Ting, D.H. Chow, and T.C. McGill, *Appl. Phys. Lett.* **57**, 2675 (1990).
- ¹³D.Z.Y. Ting, E.T. Yu, and T.C. McGill, *Phys. Rev. B* **45**, 3583 (1992).
- ¹⁴T. Takamasu, N. Miura, K. Taira, K. Funato, and H. Kawai, *Physica B* **201**, 380 (1994).
- ¹⁵J. Shen, *J. Appl. Phys.* **78**, 6220 (1995).
- ¹⁶J.F. Chen, M.C. Wu, L. Yang, and A.Y. Cho, *J. Appl. Phys.* **68**, 3040 (1990).
- ¹⁷J. Wagner, J. Schmidt, H. Obloh, and O. Koidl, *Appl. Phys. Lett.* **67**, 2963 (1995).
- ¹⁸M.S. Daly, D.M. Symons, M. Lakrimi, R.J. Nicholas, N.J. Mason, and P.J. Walker, *Semicond. Sci. Technol.* **11**, 823 (1996).
- ¹⁹E.M. Gonzalez, Y. Lin, and E.E. Mendez, *Phys. Rev. B* **63**, 033308 (2000).
- ²⁰D.H. Chow and J.N. Schulman, *Appl. Phys. Lett.* **64**, 76 (1994).
- ²¹P.C. Klipstein, S.G. Lyapin, N.J. Mason, and P.J. Walker, *J. Cryst. Growth* **195**, 168 (1998).
- ²²U.M. Khan-Cheema, Ph.D. thesis, University of Oxford (1996), pp. 42–47.
- ²³D.Z.Y. Ting, E.T. Yu, D.A. Collins, D.H. Chow, and T.C. McGill, *J. Vac. Sci. Technol. B* **8**, 810 (1990).
- ²⁴I. Lapushkin, A. Zakharova, V. Gergel, H. Goronkin, and S. Tehrani, *J. Appl. Phys.* **82**, 2421 (1997).
- ²⁵M.S. Daly, W. Lubczynski, R.J. Warburton, D.M. Symons, M. Lakrimi, K.S.H. Dalton, M. Van Der Burgt, R.J. Nicholas, N.J. Mason, and P.J. Walker, *J. Phys. Chem. Solids* **56**, 453 (1995).
- ²⁶D.M. Symons, M. Lakrimi, M. Van der Burgt, T.A. Vaughan, R.J. Nicholas, N.J. Mason, and P.J. Walker, *Phys. Rev. B* **51**, 1729 (1995).